AN UPDATE OF THE JURASSIC OPHIOLITES AND ASSOCIATED CALC-ALKALINE ROCKS IN THE SOUTH APUSENI MOUNTAINS (WESTERN ROMANIA)

Valerio Bortolotti°, Michele Marroni°°,°, Ionel Nicolae°°°, Luca Pandolfi°°,°, Gianfranco Principi*,° and **Emilio Saccani****

° *Istituto di Geoscienze e Georisorse, CNR, Italy.*
°° *Dipartimento di Scienze della Terra, Università di Pisa, 56126 Pisa, Italy.*
°°° *Institutul de Geodinamica al Academiei Romane, 79678 Bucuresti, Romania.*
* *Dipartimento di Scienze della Terra, Università di Firenze, Italy.*
** *Dipartimento di Scienze della Terra, Università di Ferrara, 44100 Ferrara, Italy.*
Corresponding Author: Emilio Saccani, e-mail sac@unife.it.

Keywords: *ophiolites, calc-alkaline, Tisza microplate, Vardar, Jurassic. South Apuseni Mts., Romania.*

ABSTRACT

This paper presents a synthesis of the researches so far carried out by the authors on the Jurassic magmatic sequences of South Apuseni Mountains. The Apuseni Mountains represent an alpine orogenic belt located in the hinterland of the Southern Carpathians. The Apuseni Mountains include a pile of basement nappes affected by Hercynian metamorphism (Bihor, Biharia, Baia de Aries, Codru nappe complexes). These nappes are overlain by an imbricated stack of tectonic units mainly consisting of Late Cretaceous clastic deposits that are, in turn, topped by the Mures nappe. This nappe includes a Middle Jurassic ophiolite sequence covered by Upper Jurassic calc-alkaline volcanics.

The ophiolite sequence consists of a gabbroic complex overlain by a sheeted dike complex and a volcanic sequence including massive and pillow-lavas. Cherts associated to pillow-lava basalts have provided Callovian to Oxfordian radiolarian associations. According to the geological and geochemical evidences, we propose that the ophiolite sequence preserved in the Southern Apuseni Mountains is representative of an oceanic lithosphere formed in a mid-ocean ridge setting.

The calc-alkaline series is mostly characterized by volcanic rocks including: basalts, basaltic andesites, andesites, dacites and rhyolites showing geochemical features typical of an intra-oceanic arc setting, and is thought to be related to Late Jurassic convergence between Eurasia and Adria plate. The calc-alkaline series is in turn overlain by Late Jurassic shallow-water limestones showing a gradual transition to Cretaceous carbonate deposits.

The geological and geochichemical features are consistent with a possible linkage of the Apuseni Mountains ophiolites with northern continuation of the Vardar oceanic domain of the Hellenic-Dinaric belt. The present-day location in the hinterland of the Carpathian area achieved in the Late Paleogene – Early Neogene time span, when the escape tectonics produced a large-scale displacement of blocks originated from the northernmost edge of the Adria plate.

INTRODUCTION

The collision of multiple microplates with the European continental margin played a major role in the formation of the collisional zones of the Alpine orogenic belts from the Alps to Carpathians. The geological evolution and geodynamic reconstruction of these microplates is generally deduced from geophysical and geological data. Among these, ophiolites are considered a useful tool for these reconstructions because they represent remnants of oceanic lithosphere originally located between converging continental plates.

In the South Apuseni Mts, located between the North Apuseni Mts and the Southern Carpathians (Western Romania), Jurassic ophiolites are widely exposed, and are always associated with Late Jurassic calc-alkaline rocks. These magmatic sequences, as well as the associated sedimentary and metamorphic rocks, are regarded as belonging to the Tisza block, a small continental microplate located behind the Carpathian belt. The complex assemblage of Jurassic ophiolitic and calc-alkaline series, as well as their magmatic affinity and their geodynamic significance have been matter of debate for long time (mostly treated in the Romanian literature). Some workers interpreted the ophiolitic sequences as fragments of a Jurassic oceanic crust developed in a mid-ocean ridge setting (Savu et al., 1981; 1994), and the calc-alkaline series as remnants of an island arc (Savu et al., 1981). By contrast, other authors suggested that the association of ophiolites with calc-alkaline rocks represents a single arc-type ophiolitic sequence (Cioflica et al., 1980; Cioflica and Nicolae, 1981; Nicolae, 1995).

In the last few years, the Jurassic magmatic associations surfacing in the South Apuseni Mountains have been object of study by the authors of this paper, who provided new stratigraphic, tectonic (Ellero et al., 2002; Bortolotti et al., 2002), and petrological (Saccani et al., 2001; Nicolae and Saccani, 2003) data on both ophiolitic and calc-alkaline sequences.

The aim of this paper is to present a synthesis and a review of data, as well as of the geological and petrological interpretations on the Jurassic magmatic sequences of South Apuseni Mountains so far individually provided in the different above-mentioned papers. The relationships between these Jurassic magmatic sequences and the geodynamic evolution of the Tisza microplate and the Carpathian belt will also be discussed.

GEOLOGICAL SETTING OF THE APUSENI MOUNTAINS

The Carpathians are an arcuate orogenic belt of Alpine age. The boundaries of the Carpathian belt are represented northward by the Eastern Alps, whereas in the southern areas it is linked with the north-south striking Hellenic-Dinaric belt (Fig. 1). The Carpathian belt originated from the Mesozoic-Cenozoic convergence motion between the European plate and the continental fragments derived from the African plate (e.g. Dercourt et al., 1990). This convergence resulted in a west-dipping subduction of the European lithosphere, that induced a large-scale crustal shortening,

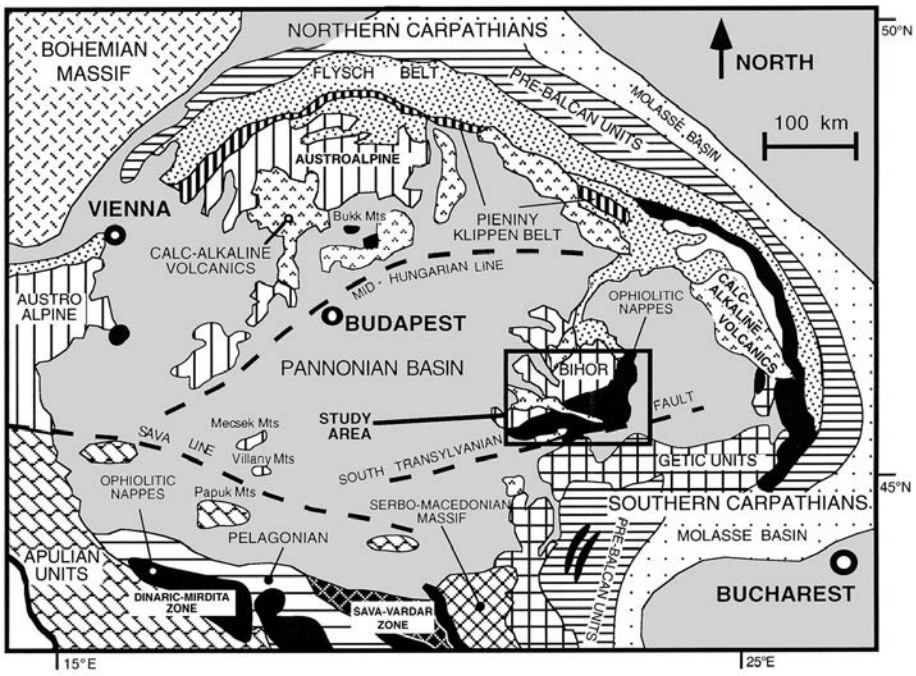

Fig. 1 - Distribution of the main geological domains in the Carpathian orogenic area (from Bortolotti et al., 2002). Box indicates the study area.

well recorded in the complex nappe stack of the Carpathian belt. This belt is mainly characterized by slices of basement and cover nappes where the record of the main Cretaceous-Neogene tectonic events is still recognizable throughout the deformation-related structures (Ratschbacher et al., 1993; Schmid et al., 1998). The shortening is accomodated by extension in the hinterland of the Carpathian belt, probably connected with an eastward retreat of the European margin (Horvath and Royden, 1981; Royden, 1993; Csontos, 1995; Linzer, 1996). This area is represented by the Pannonian area, a large sedimentary basin characterized by Neogene deposits and coeval calc-alkaline volcanites (Fig. 1). Geophysical data suggest that the substrate of the Pannonian basin is represented by an assemblage of different continental microplates, and are generally referred to as the Alcapa, Tisza and Dacia blocks. The Alcapa block is located in the northenmost area of the Pannonian basin, while the Tisza and Dacia blocks occur in the southernmost regions. The geophysical and geological data (Marton et al., 1992) suggest that the Alcapa block is separated from the Tisza block by the Mid-Hungarian line (Fig. 1), a strike-slip fault probably active since the Cretaceous. By contrast, the Tisza block is separated from the Southern Carpathians by the south Transylvanian fault (Fig. 1), regarded as a first-order tectonic line along which a dextral transpression was active in the Neogene time (e.g. Burchfiel, 1980).

The present-day location of these blocks can be explained by the escape tectonics models proposed for the Carpathian belt by Csontos (1995), Linzer et al. (1998) and Neugebauer et al. (2001). These models suggest that the continuos convergence from Cretaceous to Neogene between the Adria plate and the European plate produced shortening and thickening in the Carpathian belt. The Upper Paleogene – Lower Neogene shortening was accommodated also by the transpressive tectonics connected with the eastward escape of rigid blocks such as the Alcapa and Tisza microplates toward the Carpathian belt. This escape was driven by major strike-slip and/or transpressive faults, such as the Mid-Hungarian line or the south Transylvanian fault-system, translating the more rigid blocks toward areas where space was available. According to Csontos (1995), the escape of the Tisza microplate was probably combined with the retreat of the subducting European margin.

The outcropping structural levels of the Tisza (also known as Austro-Bihorean) microplate (Kovacs, 1982; Sandulescu, 1984) consist of crystalline and sedimentary rocks, but they are also distinguished by the most important ophiolitic sequence of the Carpathian area (Fig. 2).

The lowermost levels of the Tisza microplate are represented by tectonic units consisting of crystalline and sedimentary rocks that are mainly exposed in the Northern Apuseni Mts, where a stack of tectonic units, known as Internal Dacides, has been recognized (Fig. 2). These units are represented, from bottom to the top, by the Bihor, Codru, and Biharia complexes (Sandulescu, 1994).

In the Southern Apuseni Mts., the Biharia complex is overlain by a stack of tectonic units, mainly represented by Fenes, Grosi, Cris, Bucium, Valea Mica Galda and Bozes nappes (Blehau et al., 1981; Lupu, 1983). These nappes, reported all together as Cretaceous Flysch units in Fig. 1, are basically made up of a Cretaceous sedimentary succession consisting of coarse-grained siliciclastic deposits. In turn, the Cretaceous Flysch units are topped by the Mures nappe (Saccani et al., 2001 and quoted references). The Mures nappe includes an ophiolite sequence topped by a calcoalkaline volcanic rocks, that in turn are overlain by Late Jurassic, shallow-water carbonates (Bortolotti et al., 2002 and quoted references).

In the Bihor, Codru, and Biharia complexes a polyphase deformation history, consisting of two main Cretaceous tectonic events, has been detected. The first one ("Austrian" phase) occurred in the time spanning from Aptian to Albian, whereas the second event ("Laramian" phase) occurred during Senonian (Dallmeyer et al., 1999). The relationships between the Bihor, Codru and Biharia complexes after the "Austrian" phase are sealed by Santonian-Campanian deposits. During the "Laramian" phase, these complexes were overthrust by the Cretaceous Flysch units and the overlying Mures nappe. This phase was marked by the development of sedimentary basins filled by "Gosau" deposits of Santonian to Early Maastrichtian age. The subsequent, latest Maastrichtian to Paleocene Banatitic intrusions and related vol-

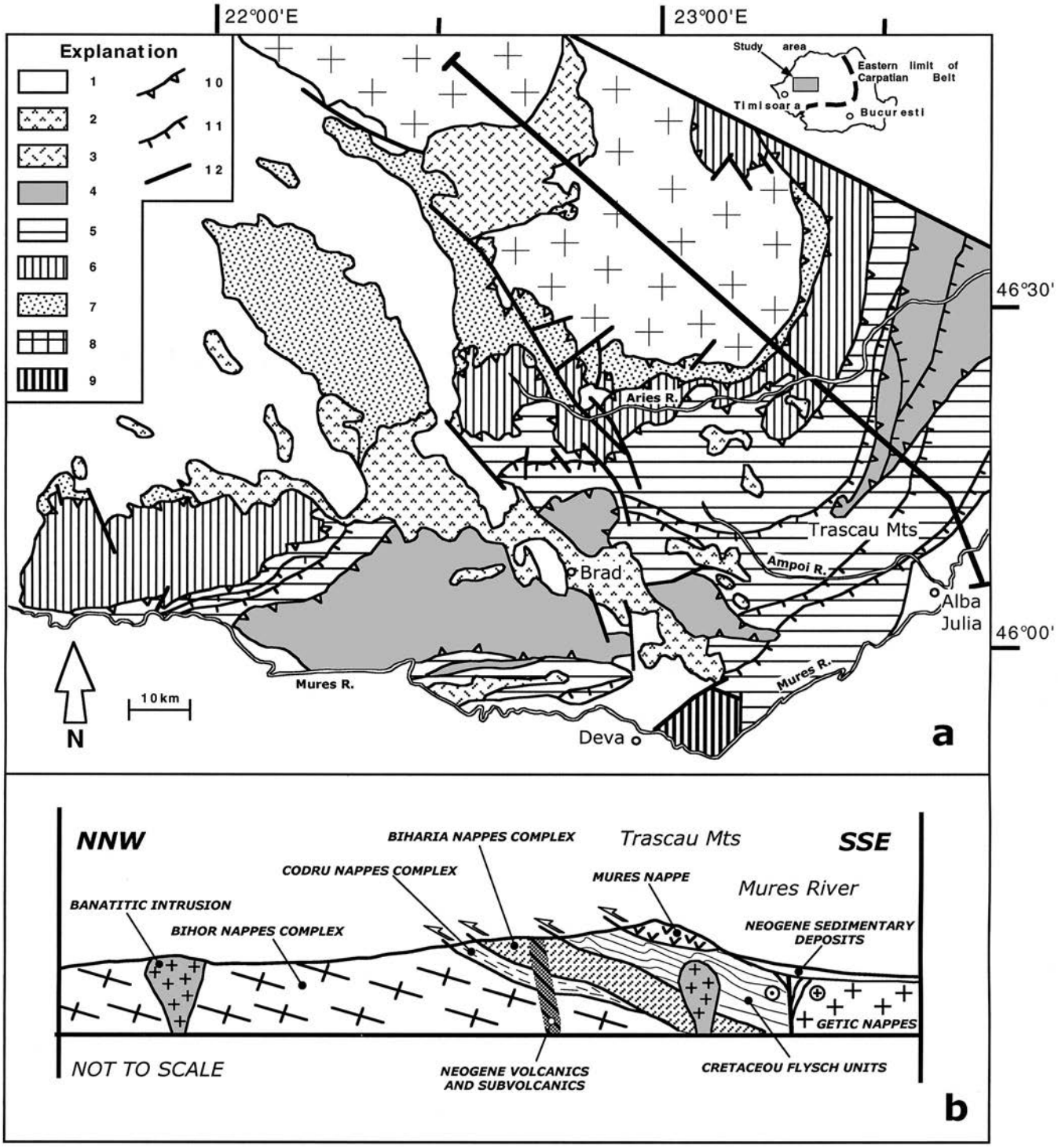

Fig. 2 - Tectonic sketch map of the eastern sector of the Apuseni Mts (a) and schematic cross section across the Trascau Mts (b); the location of the cross section is indicated in Fig. 2a.

Explanation: 1-Neogene sedimentary cover; 2-Neogene calc-alkaline intrusions and related subvolcanic rocks; 3-Banatitic intrusives and volcanics; 4-Mures nappe; 5-Cretaceous Flysch units; 6-Biharia nappes complex; 7-Codru nappes complex; 8-Bihor nappes complex; 9-Getic units; 10-Main thrusts; 11-Secondary thrusts; 12-Main faults.

canites sealed the relationships between all the tectonic units of the Apuseni Mts. The records of these deformation history has been recognized also in the Cretaceous Flysch Units. For instance, in the Fenes nappe two folding phases developed during the time spanning from Early Aptian to Late Maastrichtian have been identified (Ellero et al., 2002). The D1 phase produced WNW-verging, isoclinal to very tight folds, associated to a slaty cleavage. The main metamorphic imprint of the Fenes nappe is linked to this deformation phase; illite and chlorite "crystallinity" values indicate metamorphic conditions of the late diagenesis, close to the diagenetic-zone/anchizone boundary. The subsequent D2 phase produced NNW-verging, parallel folds, not associated with synkinematic recrystallization. These phases are interpreted as developed during a structural path that includes two phases referred to "Austrian" and "Laramian" ones. Moreover, a Jurassic tectonic event is well recorded by radiometric datings from the Biharia complex (Dallmeyer et

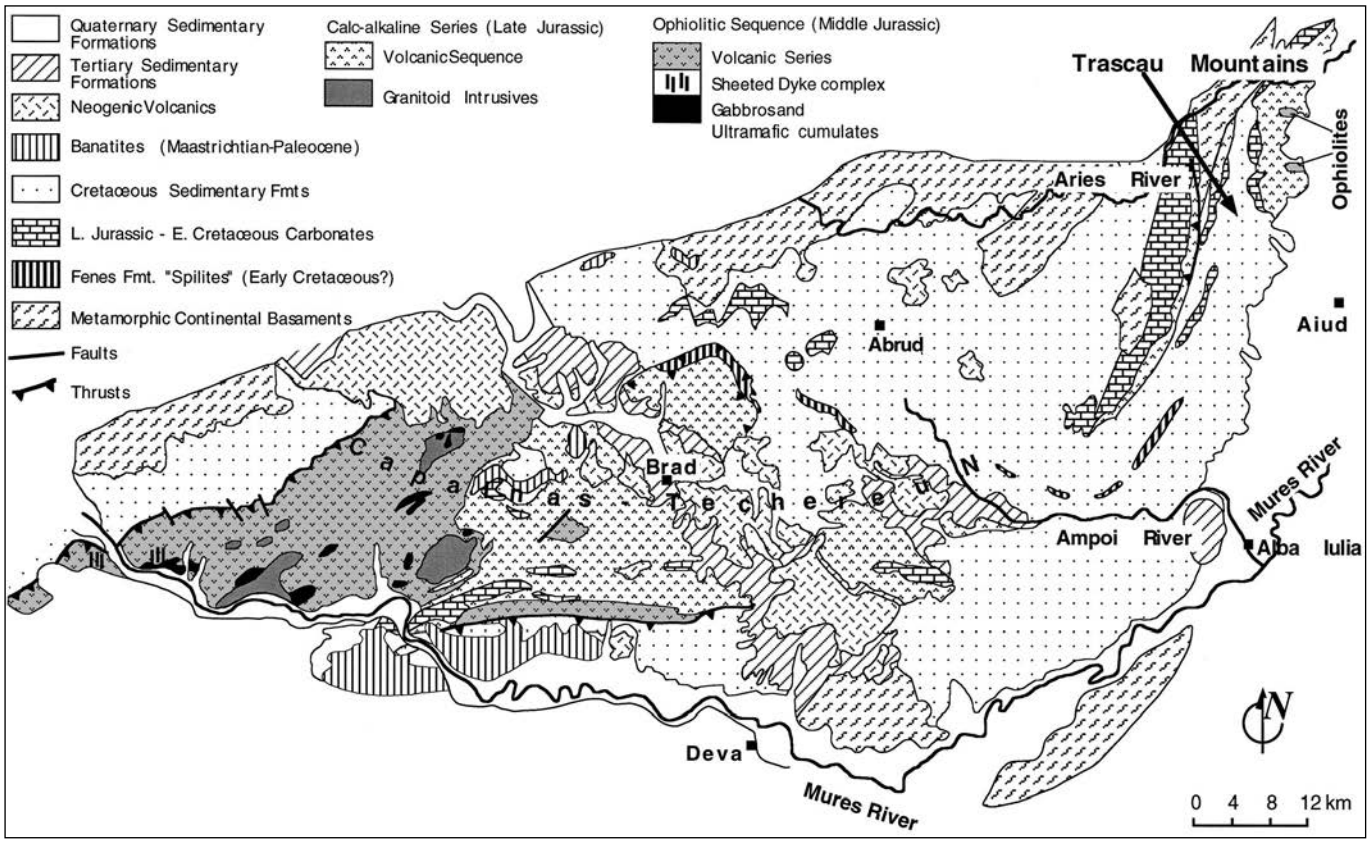

Fig. 3 - Simplified geological sketch-map of the South Apuseni Mountains. Modified after Saccani et al. (2001) and references therein.

al., 1999); this event is generally considered as related to the closure of the oceanic basin from which the South Apuseni Mts ophiolites derived (Dallmeyer et al., 1999).

GEOLOGY AND FIELD OCCURRENCE OF THE JURASSIC OPHIOLITES AND CALC-ALKALINE SERIES OF THE MURES NAPPE

The South Apuseni Mts ophiolites, which mainly crop out in the southern and southwestern sector (Fig. 3), are strongly dismembered in several tectonic slices (Lupu, 1976; Bleahu et al., 1981; Nicolae, 1995; Bortolotti et al., 2002). Consequently, although a complete sequence cannot be directly observed, a reconstruction of the pseudo-stratigraphical ophiolitic sequence (Fig. 4) can be proposed on the bases of the observed sections in the different tectonic slices. This includes an intrusive section, a sheeted dyke complex and a volcanic cover. Mantle tectonites are lacking, thus ophiolitic rocks represent only the original oceanic crust portion. The intrusive section is represented by small gabbroic bodies scattered in the south-western sector of South Apuseni Mountains (Fig. 3), and showing both layered and isostropic textures. These intrusions include very scarce ultramafic cumulates (ranging in composition from piagioclase-dunites to piagioclase-wehrlites), melagabbros, gabbros and rare gabbronorites and quarz-diorites associated with ferrogabbros (Saccani et al., 2001).

In the westernmost sector of the South Apuseni Mts (Fig. 3) gabbroic rocks are overlain by a sheeted dyke complex, characterized by parallel and sub-parallel dykes ranging in size from 10 to 50 cm. The sheeted dyke complex includes basalts, basaltic andesites and andesites.

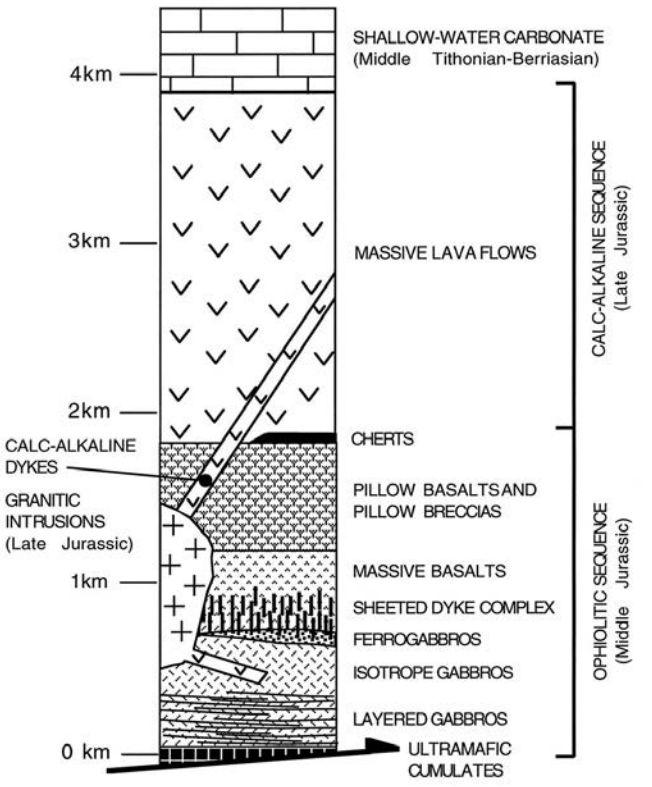

Fig. 4 - Schematic log of the Middle Jurassic ophiolite and Late Jurassic calc-alkaline sequences from the South Apuseni Mts. Relationships between ophiolites, calc-alkaline volcanics, calc-alkaline intrusions, and Upper Jurassic-Early Cretaceous sedimentary deposits are also shown. Modified after Bortolotti et al. (2002).

The volcanic sequence is by far the most abundant portion of the ophiolitic sequence (Figs. 3, 4) and includes massive and pillow-lava basalts and basaltic andesites; moreover, pillow breccias, often associated to arenites, can occasionally be found between the different lava flows.

The volcanic sequence is frequently cross cut by individual dolerite dykes. Finally, the ophiolitic sequence (Fig. 4) ends with few meters of radiolarian cherts (Nicolae et al., 1992).

The presence of more than 2 km of volcanic and subvolcanic rocks suggests that the complete ophiolitic sequence was probably very thick. Evidence of ocean-floor metamorphism in both intrusive and extrusive rocks is documented by the occurrences of actinolite and chlorite replacing primary pyroxene, and prehnite±epidote±calcite replacing plagioclase. Gabbros are also affected by secondary amphibole veinlets.

Ductile deformation and synkinematic metamorphism are absent in the South Apuseni Mts ophiolites, suggesting that their dismembering in multiple slices occurred at shallow structural levels during the orogenic tectonic phases.

Ophiolites are overlain by calc-alkaline volcanic rocks (Bleahu et al., 1981; Nicolae, 1995) (Figs. 3, 4). The calc-alkaline series (Fig. 4) is represented by massive lava flows up to 1000m-thick (with individual lava flows up to 20-30m) including basalts, basaltic andesites, andesites, dacites and rhyolites. Calc-alkaline dykes ranging in composition from andesites to dacites and rhyolites are widespread in both calc-alkaline volcanics and ophiolitic intrusive and effusive rocks (Fig. 4).

Some small calc-alkaline granitoid intrusions (Savu et al., 1996; Nicolae and Saccani, 2003) surface in the southwestern areas of the South Apuseni Mts (Fig. 3); they are largely composed of granites and granodiorites, as well as subordinate diorites, mainly found at the marginal portions of the intrusive bodies. In addition, granitic dykes and veins cut both the ophiolitic and calc-alkaline rocks (Bleahu et al., 1981; Nicolae, 1995).

In the Trascau Mts (Fig. 3), different ophiolitic-bearing units are found (Bleahu et al., 1981; Nicolae, 1995). These units mainly consist of an assemblage of slices of ophiolitic basalts and/or calc-alkaline volcanics imbricated with slices of Albian-Aptian siliciclastic turbidites.

The ages of both ophiolitic and calc-alkaline rocks are still matter of debate. A number of K/Ar datings on ophiolitic basalts have been reported by Nicolae et al. (1992), and show rather wide range of variation from 139±6 to 168±5 Ma. However, such puzzling age variations may probably be connected to perturbation phenomena due to the high heat flux associated with the intrusion of calc-alkaline dykes. Nonetheless, the oldest age (168±5 Ma), which is in agreement with the Callovian to Oxfordian radiolarian assemblages found in the associated radiolarian cherts (Lupu et al., 1995), can be assumed as the most probable age for the ophiolitic basalts, and indicate a Middle Jurassic age for the ophiolitic sequence. Available K/Ar radiometric datings for the calc-alkaline volcanics are generally unreliable (e.g. Bleahu et al., 1984 and Nicolae et al., 1987), but the age of these rocks is well constrained by the Oxfordian to lowermost Tithonian limestones intercalated in the upper part of the calc-alkaline volcanic sequence (Cioflica et al., 1981). By consequence, the age of the calc-alkaline magmatic association can be referred to the Late Jurassic, as also suggested by the 155 Ma for the associated granitoids (Pana, 1998). The calc-alkaline volcanics are overlain by a Middle Tithonian to Berriasian shallow-water carbonate sequence (Lupu, 1983). In addition, datings from ophiolites and calc-alkaline rocks highlight a short time span between the formation of these two distinct magmatic sequences.

PETROLOGY AND GEOCHEMISTRY

This section is based on the results obtained from mineral chemistry and whole-rock major oxides and trace elements analyses of about 170 samples from both ophiolitic and calc-alkaline sequences. Samples were taken in order to achieve the maximum geographical and stratigraphical coverage of the various rock types surfacing in the Capalnas-Techereu and Trascau Mountains nappes (Fig. 3). Chemical results concerning the ophiolitic rocks are presented in Saccani et al. (2001), whereas chemical data on calc-alkaline rocks are presented in Nicolae and Saccani (2003). Analytical techniques, including electron microprobe spectrometry for mineral phase analyses, and x-ray spectrometry (XRF) and inductively coupled plasma-mass spectrometry (ICP-MS) for whole-rock chemical analyses are illustrated in the above-mentioned papers together with their respective accuracy, precision and detection limits. Representative whole-rock chemical analyses are presented in Tables 1-3.

Ophiolitic sequence

The ultramafic cumulates are scarcely represented in the South Apuseni Mts ophiolites, nonetheless, they show a wide range of compositions, including olivine-websterites, plagioclase-dunites, and plagioclase-wehrlites (Saccani et al., 2001). These rocks are strongly altered, but the cumulitic textures are commonly preserved and are characterized by olivine (and, occasionally, plagioclase) as cumulus phases, and poikilitic pyroxene as intercumulus minerals. As a consequence, the crystallization order appears to be: (Cr-spinel) + olivine – plagioclase, clinopyroxene – orthopyroxene, that is, the typical MORB sequence.

The ultramafic cumulate layers show a gradual transition to gabbroic rocks, which occur in small intrusive bodies, scattered in the southwerstern part of South Apuseni Mountains. Gabbroic rocks include olivine-gabbros, gabbros, leucogabbros, scarce gabbronorites associated to Fe-gabbros, and quartz-diorites. Gabbroic rocks can be subdivided in cumulitic and isotropic types; both are characterized by crystallization order: plagioclase – clinopyroxene – orthopyroxene. Plagioclase is commonly affected by ocean-floor hydrothermal alteration; however, fresh crystals display a wide range of compositions, approximately ranging from An_{52} to An_{85} (Saccani et al., 2001). Clinopyroxene display poikilitic texture in cumulitic gabbros, whereas in isotropic gabbros is anhedral to interstitial; its composition ranges from diopside to augite, occasionally extending to endiopside (Saccani et al., 2001).

TiO_2 content in gabbros ranges from 0.43wt% to 2.58wt%, while in Fe-gabbros it is included between 2.85wt% and 3.12wt% (Fig. 5). The overall geochemical characteristics of cumulitic gabbros (Table 1) display a wide range of variation, while isotropic gabbros are characterized by less variable compositions (Saccani et al., 2001). In the latter variety, compositional changes are related to their wide degrees of fractionation (Mg#=85-64 in gabbros and 53-51 in Fe-gabbros). On the bases of their TiO_2 content and FeO/FeO+MgO ratio (Serri, 1981) gabbros show a clear high-Ti magmatic affinity (Fig. 6).

Table 1 - Representative major and trace element x-ray fluorescence analyses for the Jurassic ophiolitic rocks from the South Apuseni Mts (from Saccani et al., 2001).

	Intrusive Sequence										Sheeted Dyke Complex					
Sample	AP 3	AP114	AP109	AP111	AP125	AP177	AP 8	AP 11	AP179	AP182	AP 45A	AP123A	AP123B	AP123C	AP133B	565
Rock	Pl-Du	Pl-Wr	Gb	GbNr	Gb	Gb	Gb	Di	Fe-Gb	Fe-Gb	Bas	Bas	And	Bas	Bas	Bas
Note			Cum.	Cum.	Isotr.	Isotr.	Isotr.	Isotr.	Cum.	Cum.						
SiO_2	39.22	41.77	48.87	47.71	49.38	48.26	54.97	53.71	41.67	41.74	48.11	51.55	57.64	48.11	49.54	55.62
TiO_2	0.27	0.47	1.00	0.95	0.62	1.07	0.44	1.48	3.12	2.85	1.53	2.52	1.72	1.25	2.23	2.00
Al_2O_3	4.74	7.02	17.61	16.18	17.65	15.13	13.22	20.20	15.06	16.22	16.37	12.36	12.91	17.84	13.43	13.95
Fe_2O_3	1.31	0.00	0.99	1.07	1.04	1.27	0.78	0.41	2.04	1.97	1.46	1.72	1.59	1.33	1.66	1.38
FeO	8.74	11.53	6.60	7.13	6.93	8.50	5.21	2.76	13.63	13.13	9.73	11.48	10.60	8.88	11.05	9.17
MnO	0.15	0.18	0.14	0.12	0.13	0.14	0.16	0.06	0.20	0.20	0.17	0.16	0.11	0.16	0.15	0.16
MgO	32.98	30.04	8.22	12.95	9.47	10.24	8.78	4.40	8.65	7.92	7.01	5.77	2.78	7.33	6.87	5.82
CaO	2.19	4.06	9.53	9.51	12.67	11.62	11.70	9.16	12.80	12.81	11.01	8.34	4.72	11.03	9.62	4.25
Na_2O	0.00	0.36	3.47	1.66	1.81	1.62	2.45	4.93	1.76	1.70	2.58	4.47	6.24	2.39	3.34	5.19
K_2O	0.02	0.07	0.80	0.13	0.05	0.06	0.92	0.60	0.13	0.18	0.25	0.21	0.02	0.25	0.08	0.10
P_2O_5	0.01	0.04	0.21	0.18	0.11	0.09	0.18	0.59	0.09	0.09	0.27	0.34	0.92	0.24	0.23	0.31
L.O.I.	10.37	4.44	2.57	2.41	0.13	2.01	1.19	1.69	0.85	1.19	1.49	1.08	0.75	1.19	1.81	2.05
Total	100.00	100.00	100.00	100.00	100.00	100.00	100.00	100.00	100.00	100.00	100.00	100.00	100.00	100.00	100.00	100.00
CO_2	n.a.	n.a.	n.a.	n.a.	n.a.	n.a.	n.a.	n.a.	n.a.	n.a.	n.a.	n.a.	n.a.	n.a.	n.a.	n.a.
Mg#	87.1	84.1	68.9	76.4	70.9	68.2	75.0	74.0	53.1	51.8	56.2	47.3	31.9	59.5	52.6	53.1
Zn	72	80	50	63	50	30	49	24	83	117	93	41	29	87	37	79
Ni	1438	1010	46	250	135	63	94	31	13	18	81	25	7	92	37	7
Co	110	106	31	47	39	46	23	8	58	57	43	37	25	40	38	23
Cr	2035	2766	95	314	587	126	540	13	63	51	337	45	13	371	42	16
V	85	112	231	196	184	393	242	197	980	1069	311	487	38	256	412	251
Rb	n.d.	2	15	n.d.	2	n.d.	20	19	3	4	n.d.	n.d.	2	2	2	n.d.
Sr	8	44	272	132	108	190	300	725	220	241	129	164	47	129	162	112
Ba	29	14	263	14	10	55	235	190	20	20	50	41	17	38	38	48
Nb	n.d.	2	4	5	n.d.	3	4	9	2	3	3	9	18	5	6	7
Zr	26	43	78	72	47	32	108	99	20	34	121	191	355	102	165	217
Y	9	13	26	23	20	21	27	39	16	14	37	55	104	38	51	57

	Volcanic Sequence												Dolerite Dykes			
Sample	AP 48	AP141	AP 13	AP 40	AP 24	AP 46	AP135	AP136	AP164	AP172	AP149	AP112	AP130	AP 1	AP 25	AP151
Rock	Bas	Bas	B.And	Bas	Bas	B.And	Bas	Bas	Bas	Bas	Bas	Bas	Bas	Bas	Bas	Bas
Note	Pillow	MLF	MLF	Pillow	Pillow	MLF	Pillow	MLF	Pillow	Pillow	Pillow	Pillow				
SiO_2	39.12	48.01	53.04	45.66	47.11	53.14	47.49	47.64	48.27	50.13	46.58	48.70	48.73	46.93	47.28	47.84
TiO_2	0.92	1.05	1.84	1.49	1.00	2.05	2.63	1.82	0.89	2.01	1.08	1.46	1.44	1.65	0.86	1.25
Al_2O_3	14.79	15.24	14.44	16.19	13.79	13.34	13.91	15.72	16.76	14.39	17.08	15.54	16.00	14.58	15.46	14.80
Fe_2O_3	0.98	1.29	1.38	1.21	1.19	1.57	1.78	1.55	1.25	1.59	1.06	1.28	1.39	1.39	1.09	0.84
FeO	6.55	8.60	9.21	8.04	7.95	10.49	11.86	10.34	8.37	10.59	7.04	8.56	9.26	9.27	7.27	5.58
MnO	0.17	0.20	0.16	0.18	0.15	0.20	0.16	0.19	0.16	0.16	0.14	0.16	0.16	0.21	0.12	0.09
MgO	6.71	10.14	4.75	6.40	10.18	6.08	7.25	7.61	9.24	7.38	8.48	9.95	7.93	7.55	9.38	4.52
CaO	18.14	11.49	5.16	11.58	9.44	6.73	8.88	10.24	11.01	7.40	9.79	7.11	9.83	11.63	11.77	13.36
Na_2O	2.07	2.23	6.39	3.58	3.45	5.21	2.38	2.63	2.61	3.55	3.95	3.91	2.41	1.71	2.52	5.19
K_2O	0.53	0.05	0.60	0.96	0.16	0.10	0.17	0.29	0.12	0.07	0.53	0.31	0.08	0.05	0.20	0.79
P_2O_5	0.17	0.16	0.18	0.26	0.12	0.42	0.32	0.29	0.15	0.24	0.13	0.21	0.24	0.24	0.11	0.20
L.O.I.	9.83	1.55	2.84	4.46	5.46	0.66	3.17	1.68	1.17	2.49	4.13	2.80	2.52	4.80	3.93	5.53
Total	100.00	100.00	100.00	100.00	100.00	100.00	100.00	100.00	100.00	100.00	100.00	100.00	100.00	100.00	100.00	100.00
CO_2	7.11	n.a.	n.a.	2.17	2.85	n.a.	n.a.	0.22	n.a.	n.a.	0.82	n.a.	n.a.	n.a.	n.a.	4.36
Mg#	64.6	67.7	47.9	58.6	69.5	50.8	52.1	56.7	66.3	55.4	68.2	67.4	60.4	59.2	69.7	59.1
Zn	60	73	77	81	46	79	134	109	77	100	84	79	63	82	34	67
Ni	127	96	15	140	55	31	38	79	60	31	247	129	65	55	74	66
Co	40	44	27	41	40	32	46	43	45	40	54	42	37	43	41	21
Cr	302	346	30	354	129	85	61	270	195	37	413	336	170	107	180	275
V	193	281	445	269	287	299	445	347	256	390	195	282	302	331	255	220
Rb	3	2	6	32	3	2	n.d.	3	2	n.d.	8	7	n.d.	n.d.	3	18
Sr	213	115	114	210	172	70	120	170	107	147	294	222	144	167	187	312
Ba	79	18	79	108	52	27	23	44	23	38	105	56	54	94	69	146
Nb	2	3	6	7	3	12	8	5	n.d.	5	n.d.	7	6	4	2	n.d.
Zr	66	77	129	136	69	337	247	137	50	174	76	111	115	117	56	85
Y	25	32	38	34	32	77	68	44	30	53	24	33	41	35	23	27

Abbreviations: Pl-Du: plagioclase-dunite, Pl-Wr: plagioclase wehrlite, Gb: gabbro, GbNr: gabbronorite, Di: diorite, Fe-Gb: ferrogabbro, Bas: basalt, B.And: basaltic andesite, Cum: cumulitic texture, Isotr.: isotropic texture, MLF: massive lava flow, n.a.: not analyzed, n.d.: not detected. Fe_2O_3 / FeO = 0.15; Mg# = 100 X Mg/(Mg+Fe^{2+}), where Mg = MgO/40 and Fe = FeO/72.

Table 2 - Representative major and trace element x-ray fluorescence analyses for the Late Jurassic calc-alkaline rocks from the South Apuseni Mts (from Nicolae and Saccani, 2003, except samples marked with *.

	Intrusives				Volcanic sequence											
Sample	AP122*	AP 44	AP 38	AP 39	AP 22	AP95A	AP100	AP 37	AP 71*	V-4*	AP154	AP 91	AP156	V-3	AP158	AP157
Rock	Qz-Di	Gr-Di	Gr	Gr	Bas	Bas	Bas	B.And	B.And	B.And	B.And	B.And	B.And	And	And	And
SiO_2	59.19	68.42	71.07	74.97	44.85	48.67	53.27	51.48	52.24	53.50	54.13	54.45	54.68	55.15	55.23	56.12
TiO_2	0.81	0.31	0.34	0.18	0.60	0.89	0.76	0.55	0.55	0.58	0.54	0.47	0.46	0.57	0.43	0.51
Al_2O_3	16.43	16.24	15.27	13.96	16.17	19.68	16.83	14.94	16.46	14.06	18.08	17.40	16.96	16.09	18.28	19.13
Fe_2O_3	0.73	0.28	0.31	0.10	0.99	0.91	0.93	0.79	0.86	0.80	1.07	0.89	0.60	0.75	0.76	0.84
FeO	4.86	1.84	2.05	0.67	6.61	6.09	6.17	5.27	5.75	5.35	7.11	5.92	3.98	5.02	5.07	5.63
MnO	0.10	0.05	0.04	0.01	0.12	0.12	0.08	0.09	0.14	0.19	0.15	0.09	0.26	0.11	0.10	0.12
MgO	5.31	0.97	1.05	0.08	14.05	7.66	8.06	3.96	5.79	6.84	4.41	5.13	2.90	5.30	4.18	3.82
CaO	5.27	2.62	2.73	0.52	5.74	9.24	5.91	13.68	8.91	9.30	9.91	7.34	12.35	7.37	7.00	7.84
Na_2O	4.09	4.06	4.21	3.92	1.01	2.82	2.68	2.73	5.57	2.12	2.46	2.82	2.45	2.82	3.80	3.20
K_2O	0.74	4.43	2.08	5.03	0.68	1.23	1.68	1.35	0.13	1.45	0.24	0.96	0.66	1.36	1.15	0.54
P_2O_5	0.29	0.11	0.09	0.00	0.08	0.11	0.15	0.19	0.11	0.18	0.13	0.11	0.15	0.16	0.13	0.14
L.O.I.	2.20	0.68	0.76	0.56	9.08	2.57	3.49	4.96	3.50	5.62	1.79	4.43	4.56	5.28	3.87	2.12
Total	100.00	100.00	100.00	100.00	100.00	100.00	100.00	100.00	100.00	100.00	100.00	100.00	100.00	100.00	100.00	100.00
CO_2	n.a.	n.a.	n.a.	n.a.	3.06	n.a.	n.a.	3.39	n.a.	1.64	n.a.	n.a.	2.62	n.a.	0.66	n.a.
Mg#	66.07	48.4	47.8	17.4	79.1	69.15	69.95	57.2	64.2	69.5	52.48	60.7	56.47	65.3	59.55	54.77
Pb	2	4	11	4	20	4	7	10	6	8	9	7	8	12	4	10
Zn	40	26	26	12	97	55	51	44	51	57	73	71	57	59	59	67
Ni	7	3	n.d.	n.d.	223	89	44	61	41	78	30	18	26	62	21	15
Co	14	4	2	n.d.	38	31	25	24	22	23	32	22	20	22	20	17
Cr	13	9	7	5	550	303	81	265	63	267	73	43	38	154	32	26
V	124	46	42	13	241	168	258	196	324	168	248	212	195	142	176	193
Rb	5	132	64	174	19	27	36	19	2	19	2	12	9	27	19	8
Sr	344	866	302	160	217	334	405	458	322	323	512	419	283	404	294	330
Ba	94	1485	427	636	141	249	196	247	50	149	110	119	123	215	212	107
Th	3	43	11	38	8	n.d.	6	4	5	5	n.d.	5	n.d.	10	3	3
Nb	7	14	6	20	10	n.d.	2	5	n.d.	5	n.d.	2	2	6	n.d.	n.d.
Zr	201	200	152	142	70	62	100	89	44	107	64	85	60	144	86	86
Y	43	18	17	5	16	23	21	16	17	19	15	16	15	24	17	21

	Volcanic sequence							Dykes in calc-alkaline				Dykes in ophiolites				
Sample	AP95B	V-14	AP99	AP 21	AP97	501	AP96A	AP 72	457*	459	AP159	AP 49	AP 32	AP101*	AP 30	AP 7
Rock	And	And	Dac	Dac	Rhy	Rhy	Rhy	Bas	And	And	And	Bas	B.And	And	Dac	Mic-Gr
SiO_2	59.78	60.07	63.57	64.15	69.98	70.05	75.34	48.27	57.66	59.54	62.24	46.31	52.38	56.26	61.29	71.44
TiO_2	0.93	0.73	0.75	0.54	0.34	0.32	0.27	0.79	0.90	0.62	0.59	0.41	0.72	0.72	0.32	0.33
Al_2O_3	17.78	15.82	15.49	16.18	15.12	13.28	12.26	17.81	16.44	16.64	16.86	17.75	15.73	18.75	18.60	14.67
Fe_2O_3	0.76	0.68	0.48	0.51	0.29	0.43	0.16	1.18	0.81	0.68	0.63	0.86	0.85	0.70	0.36	0.28
FeO	5.10	4.54	3.21	3.41	1.96	2.85	1.04	7.87	5.38	4.54	4.20	5.73	5.63	4.69	2.43	1.85
MnO	0.11	0.21	0.08	0.10	0.05	0.09	0.03	0.14	0.15	0.11	0.08	0.05	0.11	0.08	0.04	0.02
MgO	3.82	3.62	3.72	2.45	0.53	2.56	0.30	8.97	4.33	3.73	2.97	2.01	7.73	4.32	1.26	0.72
CaO	2.09	6.81	6.25	2.15	1.67	4.01	1.74	6.06	5.73	4.23	2.73	22.55	5.82	2.05	3.70	1.86
Na_2O	3.89	3.42	2.97	4.80	3.35	3.33	3.19	4.04	3.62	3.25	4.41	0.02	4.02	6.57	4.53	4.01
K_2O	2.55	1.59	1.47	3.95	6.00	1.12	3.42	1.06	0.70	2.70	3.12	0.01	1.33	2.42	2.59	4.12
P_2O_5	0.23	0.18	0.18	0.15	0.10	0.05	0.08	0.15	0.26	0.16	0.19	0.18	0.14	0.15	0.17	0.06
L.O.I.	2.97	2.34	1.84	1.63	0.60	1.91	2.18	3.67	4.03	3.80	1.98	4.12	5.55	3.28	4.69	0.64
Total	100.00	100.00	100.00	100.00	100.00	100.00	100.00	100.00	100.00	100.00	100.00	100.00	100.00	100.00	100.00	100.00
CO_2	0.54	n.a.	0.23	n.a.	n.a.	n.a.	1.36	n.a.	n.a.	n.a.	n.a.	n.a.	n.a.	0.41	n.a.	n.a.
Mg#	57.17	58.7	67.38	56.1	32.62	61.5	33.92	67.0	58.9	59.4	55.76	38.5	71.0	62.11	48.1	41.2
Pb	7	10	12	28	8	10	7	5	8	8	11	7	10	7	13	9
Zn	60	48	39	53	33	41	34	70	71	58	55	11	78	46	27	16
Ni	47	36	38	n.d.	4	6	4	80	10	10	18	18	56	13	n.d.	4
Co	16	18	20	7	4	9	4	38	18	15	13	8	26	15	4	5
Cr	95	75	63	4	12	23	12	236	15	19	21	51	161	13	3	10
V	99	186	183	59	42	101	43	296	119	107	94	216	166	189	32	22
Rb	91	25	26	63	115	22	73	19	10	67	68	n.d.	33	62	71	130
Sr	291	392	393	175	164	182	180	360	306	257	249	12	358	275	312	233
Ba	615	243	264	513	350	284	353	201	185	521	363	46	406	248	416	622
Th	7	7	4	12	10	6	8	3	12	11	11	n.d.	5	7	7	18
Nb	16	7	3	7	3	4	5	2	59	34	3	3	5	2	7	7
Zr	197	126	119	167	166	108	158	62	350	255	157	36	134	117	193	211
Y	22	23	28	26	17	17	18	24	38	32	24	13	25	25	20	20

Abbreviations- Qz-Di: quartz diorite, Gr-Di: granodiorite, Gr: granite, Bas: basalt, B.And: basaltic andesite, And: andesite, Dac: dacite, Rhy: rhyolite, Mic-Gr: micro-granite, n.a.: not analyzed, n.d.: not detected. Fe_2O_3 / FeO = 0.15; Mg# = 100 X Mg/(Mg+Fe^{2+}), where Mg = MgO/40 and Fe = FeO/72.

Table 3 - Representative inductively coupled plasma-mass spectrometry trace element analyses for the Jurassic ophiolitic rocks (from Saccani et al., 2001) and Late Jurassic calc-alkaline rocks and from the South Apuseni Mts (from Nicolae and Saccani, 2003) from the South Apuseni Mts.

	Ophiolites								Calc-alkaline						
Sample	AP 45A	AP123A	AP123C	AP 13	AP135	AP136	AP 1	AP151	AP 22	AP 37	AP154	AP 91	AP156	V-3	AP157
Rock	Bas	Bas	Bas	B.And	Bas	Bas	Bas	Bas	Bas	B.And	B.And	B.And	B.And	And	And
Note	Sh-Dy	Sh-Dy	Sh-Dy	MLF	Pillow	MLF	Dyke	Dyke	MLF	MLF	MLF	MLF	MLF	MLF	MLF
Sc	92.4	93.5	99.1	81.1	111	105	88.7	76.5	59.9	53.6	67.4	61.1	80.30	61.4	59.80
Nb	2.97	6.94	2.71	2.91	7.63	4.03	3.37	1.33	1.11	4.18	1.54	1.79	1.44	3.78	2.34
Hf	3.01	3.80	2.72	3.75	7.92	3.39	2.96	2.09	1.62	2.58	1.86	2.22	1.61	3.31	2.36
Ta	0.26	0.62	0.23	0.36	0.62	0.35	0.94	0.36	0.15	0.42	0.23	0.19	0.17	0.35	0.20
Th	0.19	0.66	0.16	0.55	0.68	0.25	0.23	0.32	2.25	5.14	1.68	2.96	2.31	5.9	2.45
U	0.08	0.19	0.06	0.34	0.31	0.09	0.08	0.33	0.60	1.58	0.76	0.74	1.21	1.92	0.64
La	3.62	8.94	3.78	4.45	10.3	5.41	3.85	3.17	3.47	12.4	5.16	7.25	7.71	15.9	6.96
Ce	12.2	25.9	12.1	13.9	31.5	17.0	12.2	10.8	9.40	29.3	15.2	15.6	17.8	35.9	17.2
Pr	1.89	4.10	1.99	2.21	5.03	2.75	1.87	1.59	1.33	3.43	1.57	2.2	2.24	4.32	2.20
Nd	10.2	21.6	10.8	11.9	26.5	14.9	10.2	8.39	6.20	14.3	6.72	9.74	9.39	17.7	9.81
Sm	3.53	6.84	3.81	4.00	8.63	4.94	3.36	2.69	1.62	3.06	1.66	2.34	2.44	3.97	2.44
Eu	1.24	2.23	1.37	1.36	2.74	1.73	1.25	0.97	0.53	0.87	0.53	0.75	0.77	1.15	0.74
Gd	4.25	8.40	4.59	4.97	10.5	6.24	4.23	3.09	1.66	2.90	1.61	2.35	2.30	3.6	2.42
Tb	0.85	1.61	0.92	1.00	2.05	1.20	0.83	0.57	0.28	0.41	0.25	0.37	0.36	0.53	0.39
Dy	5.71	10.7	5.98	6.77	13.2	7.69	5.78	3.72	1.76	2.47	1.55	2.36	2.22	3.07	2.47
Ho	1.26	2.22	1.27	1.47	2.83	1.61	1.25	0.75	0.36	0.50	0.30	0.49	0.45	0.58	0.52
Er	3.71	6.51	3.80	4.46	8.59	4.77	3.64	2.19	1.10	1.48	0.91	1.51	1.38	1.8	1.60
Tm	0.50	0.88	0.50	0.60	1.15	0.64	0.51	0.28	0.16	0.19	0.13	0.21	0.19	0.24	0.23
Yb	3.59	5.92	3.53	4.29	8.00	4.41	3.55	1.99	1.10	1.41	0.94	1.56	1.39	1.83	1.71
Lu	0.52	0.83	0.52	0.60	1.17	0.65	0.52	0.28	0.17	0.21	0.15	0.23	0.21	0.27	0.27

Abbreviations- Bas: basalt, B.And: basaltic andesite, And: andesite, Sh-dy: sheeted dyke, MLF: massive lava flow.

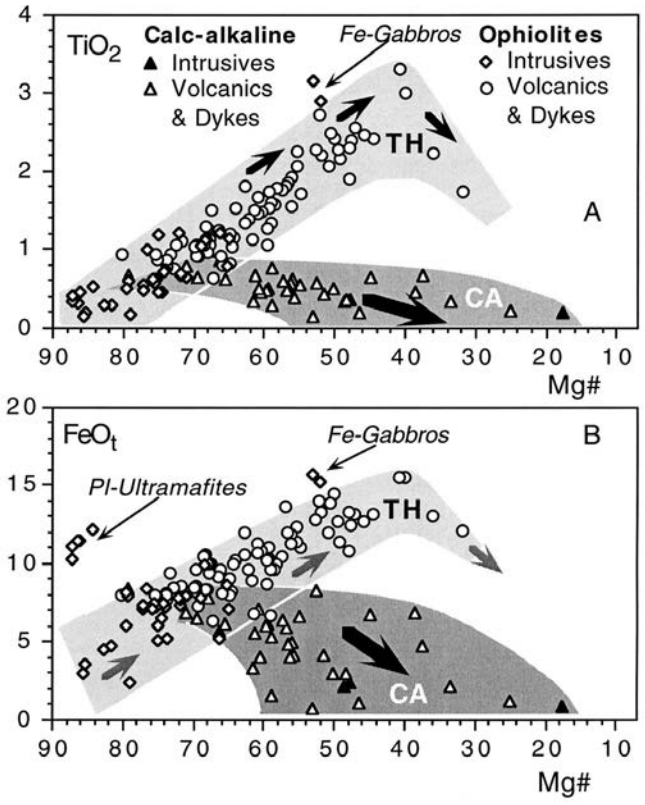

Fig. 5 - TiO_2 (A) and FeO_t (B) variations in relation to Mg# variation for Middle Jurassic ophiolitic and Late Jurassic calc-alkaline rocks from the South Apuseni Mts. TH: tholeiitic trend, CA: calc-alkaline trend.

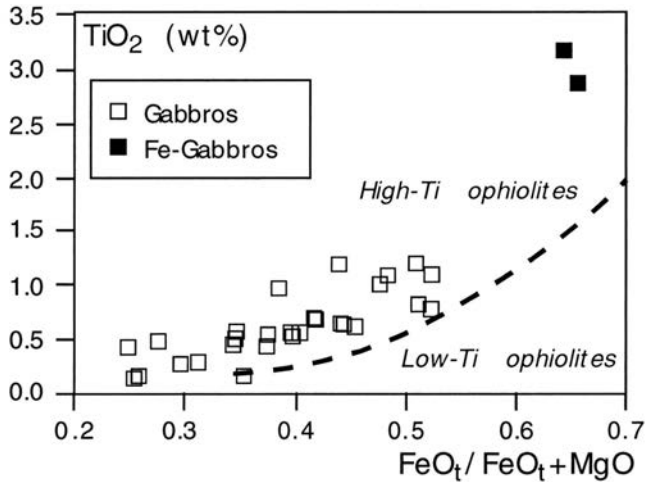

Fig. 6 - TiO_2 vs. FeO_t/FeO_t+MgO discrimination diagram for the South Apuseni Mts ophiolitic gabbros. The dashed line separates the fields for high-Ti and low-Ti ophiolites. Modified after Serri (1981).

The sheeted dyke complex is largely dominated by basalts, whereas basaltic-andesites and andesites are subordinate. Dykes reveal different textures, ranging from fine- to medium-grained aphyric to plagioclase porphyritic types with intergranular to doleritic textures and one-way vitrophyric chilled margins. Fresh mineralogical phases of basaltic dykes show chemical compositions very similar to those of MOR basalts (Saccani et al., 2001), as exemplified by the clinopyroxene compositions plotted in the discrimination diagrams of Fig. 7. Plagioclase displays a wide range of compositions (about An_{50}-An_{87}). In addition, chemical variations between different crystals within a sample and from core to rim of individual crystals is considerable. These chemical variations are in accordance with the continuous supply of primitive melts in the magma chamber in a MOR setting. Dykes are chemically characterized by high contents of high field strength elements (HFSE) such as: TiO_2 (1.25wt% - 3.24wt%), P_2O_5 (0.23wt% - 0.41wt%), Y (38ppm – 75ppm) and Zr (102ppm – 287ppm), with Mg# ranging from 60.8 to 46. Compatible element abundance (Cr = 33ppm - 370ppm, Ni

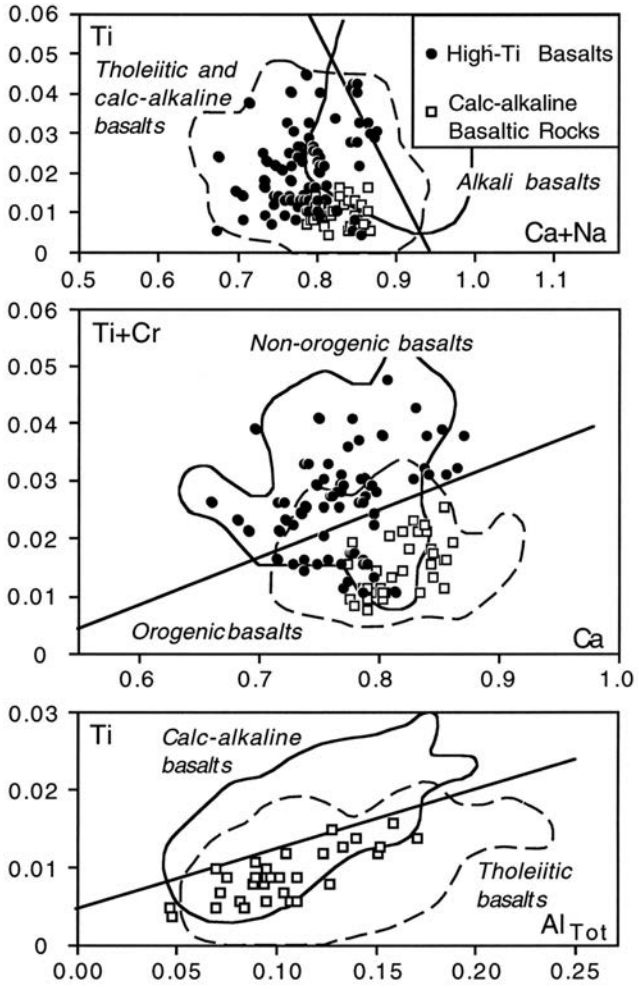

Fig. 7 - Clinopyroxene discrimination diagrams for South Apuseni Mts ophiolitic and calc-alkaline basaltic rocks. Modified after Leterrier et al. (1982).

= 20ppm - 92ppm) suggest that these magmas are generally slightly differentiated.

Their overall geochemical characteristics indicate a clear high-Ti magmatic affinity, as also testified by the Ti/V discrimination diagram (Fig. 8), as well as by the incompatible element concentrations shown in Fig. 9a, which display the typical flat patterns from Nb to Yb, with respect to N-MORB composition. Rare earth elements (REE) display both concentrations (Table 3) and chondrite-normalized flat patterns (Fig. 10a) very similar to those observed in normal MORBs.

The volcanic sequence and related individual dolerite dykes are largely characterized by basalts, whereas basaltic andesites are subordinate and andesites are very rare. Texturally, these rocks are commonly aphyric to moderately porphyritic, with intersertal, intergranular and ophitic to subophitic groundmass (Saccani et al., 2001). Likewise other ophiolitic rocks, most of the samples from the volcanic sequence are hydrothermally metamorphosed, with plagioclase and clinopyroxene variably replaced by albite and by actinolite-hornblende, respectively. However, fresh plagioclase ranges from An_{55}-An_{85}, and fresh clinopyroxene show chemical compositions very similar to those of clinopyroxene from MORBs (Beccaluva et al., 1989, Leterrier et al., 1982) (Fig. 7). Basaltic rocks show a wide range of geochemical compositions (Table 1), as well as fractionation extent (Mg#=70-40). Compared with the sheeted dykes, lavas show lowest degree of fractionation (Fig. 8), as well as lower contents in HFSE. Nevertheless, the FeO and TiO_2 increase during fractionation (Fig. 5), as well as the flat N-MORB-normalized incompatible element patterns (Fig. 9a) are consistent with the compositions of Mid Ocean Ridge basalts. Accordingly, their high-Ti (MORB) geochemical affinity is also clearly indicated by the TiO_2 content (0.73-2.98wt%), P_2O_5 (0.13-0.42wt%), Y (20-68ppm) and Ti/V ratios (20-40, Fig. 8). REE compositions (Table 3) display typical MORB concentrations with chondrite-normalized REE patterns rather flat or slightly enriched in light-REE with respect to medium- and heavy-REE (Fig. 10a). On the whole, $(La/Sm)_N$ ratios vary from 0.75 to 1.11, while $(La/Yb)_N$ ratios are included between 0.85 and 1.69. Only the most primitive analyzed sample displays light-REE depletion relative to medium- and heavy-REE, with $(La/Sm)_N$ = 0.62, $(La/Yb)_N$ = 0.68, and $(Sm/Yb)_N$ = 1.09 (Saccani et al., 2001). REE abundances reflect various degrees of fractionation, ranging from about 10 to 50 times chondritic abundance. In the more evolved samples Eu negative anomalies are observed (Fig. 10a), reflecting previous removal of early crystallized plagioclase. In summary, the REE patterns suggest the occurrence of both N-type and transitional-type MORBs.

The definite similarity in incompatible element abundance between sheeted dykes and volcanics (Figs. 9a, 10a) indicate a strict co-genetic origin for these rocks. In summary, as already outlined by Saccani et al. (2001), all the data suggest that the South Apuseni Mts. ophiolites were generated in a mid-ocean ridge setting.

Calc-alkaline series

Representative chemical analyses of South Apuseni Mts calc-alkaline intrusive, volcanic and subvolcanic rocks are presented in Tables 2, 3. Calc-alkaline intrusives, range in composition from micro-diorites to granodiorites and granites, and are found as small plutonic bodies scattered throughout the ophiolitic series in the southwestern part of

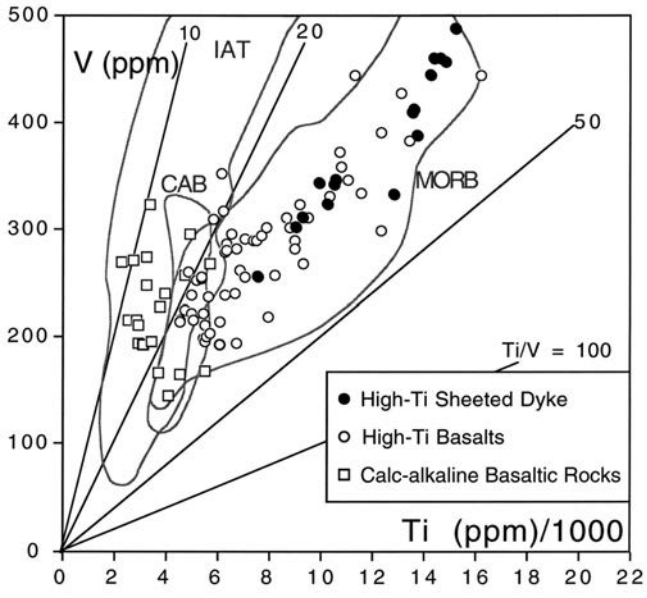

Fig. 8 - V vs. Ti/1000 discrimination diagram for ophiolitic and calc-alkaline mafic volcanic rocks from South Apuseni Mts. Compositional fields proposed by Shervais (1982) are shown: IAT = island arc tholeiites, CAB = calc-alkaline basalts, MORB = mid-ocean ridge basalts.

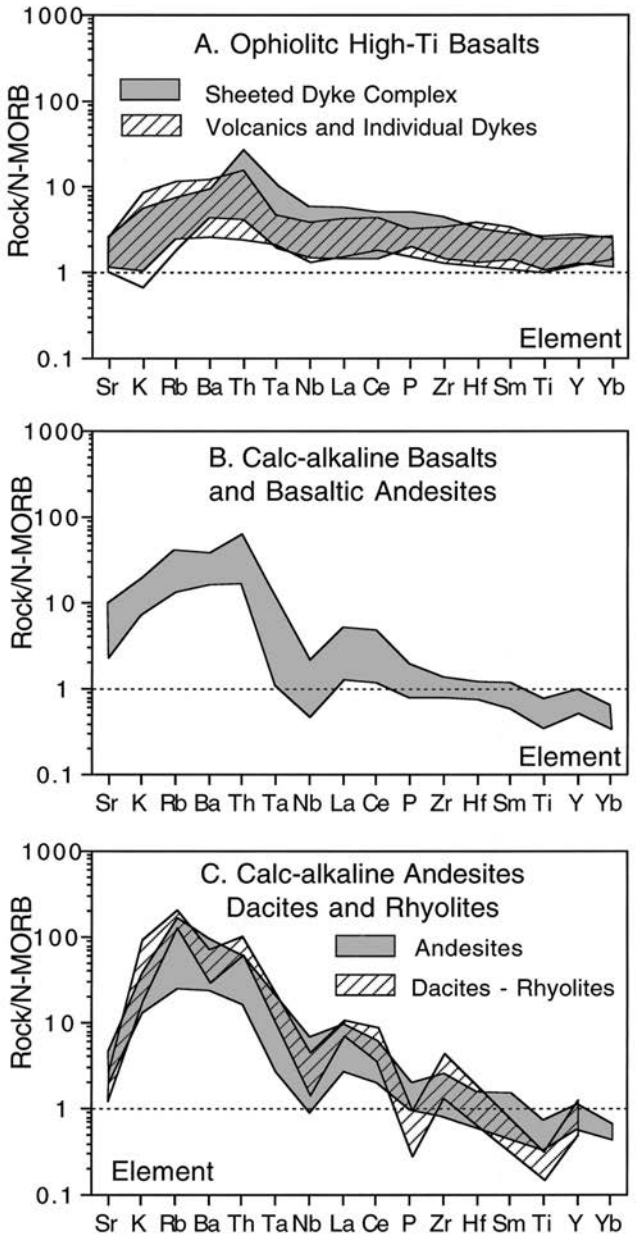

Fig. 9 - N-MORB-normalized incompatible element patterns for the South Apuseni Mts Jurassic magmatic associations. Normalizing values are from Sun and McDonough (1989). A: high-Ti ophiolitic basalts, B: calc-alkaline basalts and basaltic andesites, C. calc-alkaline andesites, dacites, and rhyolites.

the Mures nappe (Fig. 3). Calc-alkaline volcanic and sub-volcanic rocks show a typically wide compositional range, including basalts, basaltic andesites, andesites, dacites and rhyolites, with basaltic andesites largely predominating in the volcanic sequence, and andesites, dacites and rhyolites prevailing in dykes. Nicolae and Saccani (2003) pointed out that both volcanic and sub-volcanic rock exhibit a clear calc-alkaline affinity (according to the classification diagram shown in Fig 11: Miyashiro, 1974).

All volcanic and subvolcanic rocks characteristically have highly porphyritic textures, where the phenocryst assemblage is dominated by clinopyroxene, orthopyroxene and plagioclase, as well as Mg-hornblende in the more evolved rocks, i.e., from basaltic andesites to rhyolites. Groundmasses are vesiculated intergranular to hyalopilitic in basaltic and andesitic rocks, and hyalopilitic in dacites and rhyolites.

In basalts and basaltic andesites, compositions of plagioclase phenocrysts are greatly variable (An_{80}-An_{68}), while groundmass plagioclase microlites have significantly lower An contents (An_{53}-An_{50}). In addition, plagioclase phenocrysts show both normal and reverse zoning (Nicolae and Saccani, 2003).

Clinopyroxene phenocrysts from the basalts and basaltic andesites are considerably subalkaline, and are similar to those of the calc-alkaline basalts described by Leterrier et al. (1982) (Fig. 7). They generally range from diopsidic to augitic and Mg-rich augitic compositions and are generally characterized by reverse zoning (Nicolae and Saccani, 2003).

In the Ti/1000 vs. V diagram of Fig. 8 (Shervais, 1982) calc-alkaline basalts plot in the compositional fields for calc-alkaline and island arc basalts. Nicolae and Saccani (2003) have shown that N-MORB-normalized incompatible element patterns for calc-alkaline basalts and basaltic andesites (Fig. 9b) show the typical patterns of oceanic calc-alkaline basaltic rocks (Pearce, 1983) characterized by Ta-Nb and Ti negative anomalies, as well as Rb-Ba-Th and La-Ce positive anomalies. Both these positive and negative anomalies increase in magnitude in andesites, dacites, and rhyolites, where significant P negative anomaly and Rb positive anomaly can also be observed (Fig. 9c). The calc-alkaline differentiation trend is also testified by the sharp decreasing of TiO_2 and FeO_t with increasing SiO_2 (Fig. 5), which reflect the crystallization of Fe-Ti oxides in the early stages of magmatic evolution. In adddition, the studied rocks show decreasing abundances of HFSE, such as P, Zr, and Y, with increasing SiO_2. The enrichment of LFSE relative to HFSE (Figs. 9b, c) is related to the enrichment of the mantle sources by LILE-enriched fluids derived from the subducted oceanic crust.

Calc-alkaline basalts and basaltic andesites exhibit marked light REE enrichments with respect to HREE (Fig. 10b), exemplified by the $(La/Yb)_N$ ratios = 2.3 - 6.3; these enrichments are commonly interpreted as a consequence of mantle source enrichment by subduction-derived components.

Nicolae and Saccani (2003) have demonstrated that the main evolutionary process responsible for rock differentiation in the calc-alkaline series was simple fractional crystallization in closed systems. This conclusion is supported by many evidences: (1) both plagioclase and clinopyroxene phenocrysts are in equilibrium or near-equilibrium with the bulk composition of their host rocks; (2) trace element variations display very good correlation with silica and are consistent with fractionation of the observed phenocryst minerals; (3) very constant LILE/HFSE ratios allow to exclude possible contribution of the lower crust to magma composition (e.g., assimilation-fractional criystallization: DePaolo, 1981).

Nicolae and Saccani (2003) suggested that the South Apuseni Mountains Jurassic calc-alkaline series originated from primary melts derived, in turn, from a depleted mantle source enriched in LILE (high Ba/Y ratios) and LREE (Fig. 10b) by slab-derived hydrous fluids. According to Hildreth and Moorbath (1988), high HFSE/LFSE ratios (e.g., Zr/Th = 10 - 40) indicate that these rocks formed in an intra-oceanic arc setting. Pressures of formation, estimated from phenocryst assemblages, are about 1.8-2.3 kbar, while temperatures range from 1216°C in basaltic rocks to 860°C in rhyolites (Nicolae and Saccani, 2003).

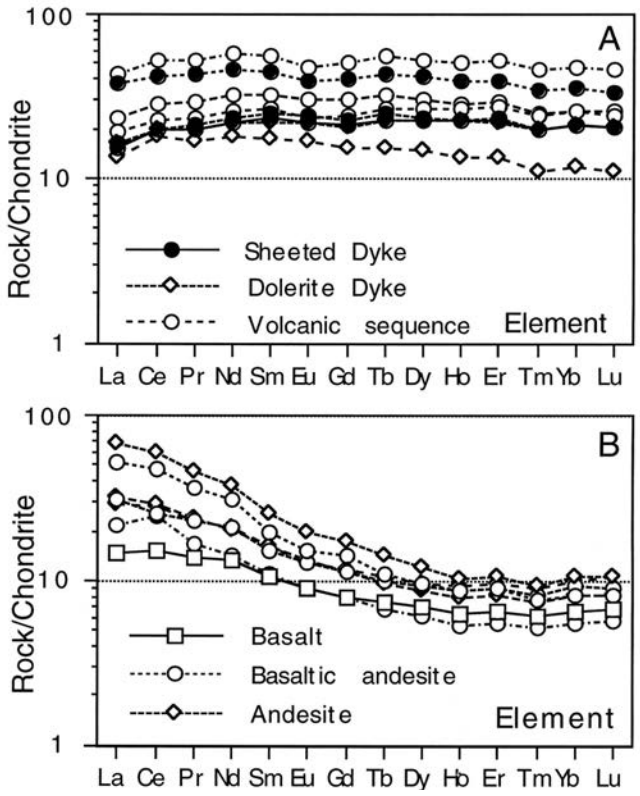

Fig. 10 - Chondrite-normalized REE patterns for the South Apuseni Mts Jurassic magmatic associations. Normalizing values after Sun and McDonough (1989). A: ophiolitic high-Ti basalts and basaltic andesites, B: calc-alkaline basalts, basaltic andesites, and andesites.

DISCUSSION

The review presented in this paper highlight the occurrence in the South Apuseni Mts of Middle Jurassic ophiolites, showing mid-oceanic ridge affinity; these ophiolites are, in turn, overlain by Upper Jurassic island arc calc-alkaline magmatic sequences. The data presented in this paper suggest that the Upper Jurassic geodynamic framework of the area in which the Apuseni Mts ophiolites originated was characterized by a calc-alkaline volcanic sequences developed over an older MOR oceanic lithosphere (Bortolotti et al., 2002). The reconstruction of the geodynamic history includes a development in the Middle Jurassic of MOR oceanic lithosphere that subsequently became trapped in a supra-subduction zone where the calc-alkaline volcanic sequences were emplaced in the Late Jurassic. This reconstruction implies that the oceanic area was affected by convergence, with development of subduction zone at the boundary between the Middle and the Late Jurassic, as testified by the occurrence of the Late Jurassic calc-alkaline volcanic sequences.

In the geodynamic reconstruction proposed for Carpathian area (Sandulescu, 1994; Csontos, 1995; Dal Piaz et al., 1995; Schmid et al., 1998; Zacher and Lupu, 1998; Bortolotti et al., 2002 and many others), the oceanic basin, from which the South Apuseni Mts ophiolites were originated, was located in an area, characterized by several amalgamated continental blocks located at the northernmost edge of the Adria plate. These blocks were separated from the European plate by small oceanic domains referred to the two main branches of the Tethys, i.e. the Ligure-Piemontese and Vardar oceanic basins, very close to each other.

The re-examination of previously published data presented in this paper allow to discriminate if the Apuseni Mts ophiolites were most likely originated in the Ligure-Piemontese or Vardar oceanic basin.

Many characteristics of the ophiolite sequence from the South Apuseni Mountains, such as the presence of a well developed sheeted dyke complex and the relevant thickness of the basalts (up to 2 km thick) are similar with those of the ophiolites from the Sava-Vardar Zone of the Hellenic-Dinaric belt (e.g. Lugovich et al., 1991; Pamic et al, 2002 and quoted references). The very thin level of radiolarian cherts as the only ophiolitic sedimentary cover is a further feature that can commonly be recognized in the MORB ophiolites of the Hellenic-Dinaric belt. Further evidences are provided by the occurrence of Callovian to Oxfordian radiolarites coherent with the age detected for the radiolarites from the Guevgueli ophiolites from Vardar oceanic basin (Danelian et al., 1996). These radiolarites are older than the deposits generally found at the top of the Ligure-Piemontese ophiolites (e.g. Abbate et al., 1986). Moreover the occurrence of Middle Tithonian to Berriasian shallow-water carbonate deposits (Lupu, 1983) at the top of the sequence is a typical feature of the Sava-Vardar Zone ophiolites. Generally, these shallow-water carbonates are interpreted as deposited over the ophiolites after their obduction (e.g. Robertson, 1994). This occurrence suggests that the South Apuseni Mts ophiolites were already emplaced during the Late Jurassic, as generally accepted in the reconstruction proposed for the Hellenic-Dinaric belt ophiolites. By contrast, the Ligure-Piemontese ophiolites never display any indications of convergence-related events of Late Jurassic age (Abbate et al., 1980). But, a significant evidence for this correlation is provided by the close association of these ophiolites with the Late Jurassic calc-alkaline volcanics and related granitoids. This setting strongly resembles the geological setting of the Fanos area (Bébien et al., 1987), where MOR basaltic rocks are intruded by Late Jurassic calc-alkaline granites.

Another striking evidence for close similarities between the South Apuseni Mts and Sava-Vardar Zone ophiolites can be observed for the geochemistry of mafic rocks. Saccani et al. (2001) and Bortolotti et al. (2002) have demonstrated close geochemical analogies between South Apuseni Mts gabbros and gabbros from the Sava-Vardar Zone of the Dinaric belt (Ivanov et al., 1987; Lugovich et al., 1991; Trubelja et al., 1995). These authors have also shown close compositional analogies, expressed in terms of

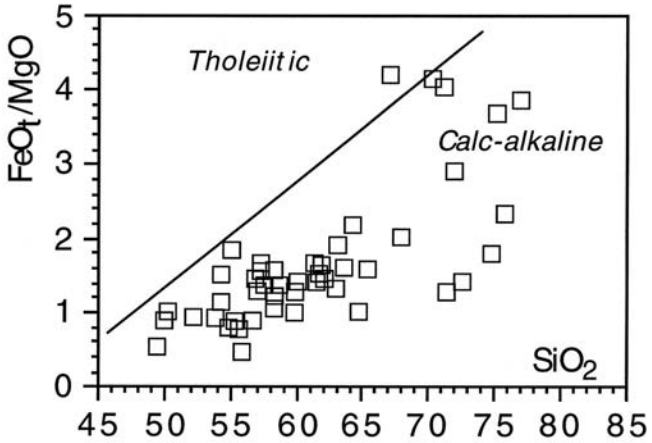

Fig. 11 - FeO_t/MgO vs. SiO_2 (wt%) discrimination diagram for the South Apuseni Mts calc-alkaline volcanic rocks. Modified after Miyashiro (1974).

incompatible element abundances, between South Apuseni Mts and Sava-Vardar Zone (Lugovich et al., 1991; Trubelja et al., 1995) ophiolitic basalts. However, the most convincing evidence of strict geochemical similarities between these two ophiolitic series is provided by the REE contents displayed by both subvolcanic and volcanic basaltic rocks (Fig. 10a). In fact, most high-Ti basalts from the South Apuseni Mts ophiolites, though showing various degrees of fractionation (LREE = 10-50 times chondritic abundance), are characterized by characteristically flat or slightly LREE-enriched chondrite-normalized REE patterns. The $(La/Yb)_N$ ratios can be used for summarizing the LREE/HREE relative enrichments. In high-Ti basalts from South Apuseni Mts this ratio varies (with the exception of a rather primitive basalt) from 0.85 to 1.69, with an average value of 1.19. Although some LREE depleted basalts are present, similar REE patterns are displayed by most of the high-Ti basalts from the Sava-Vardar Zone ophiolites (Lugovich et al., 1991; Trubelja et al., 1995), which are characterized by $(La/Yb)_N$ ratios averaging 1.12 (Lugovich et al., 1991) and 0.96 (Trubelja et al., 1995).

By contrast, high-Ti basaltic rocks from the Eastern Alps, Northern Apennine Internal Ligurides, as well as from the Dinaride Ophiolite Zone (Dinarides) and Mirdita Zone (Albanides) are characterized by noticeable relative depletion of LREE with respect to HREE. The $(La/Yb)_N$ ratios displayed by the Eastern Alps (Venturelli et al, 1981) and Mirdita (our unpublished data) ophiolitic basalts are always lower than 0.81 and 0.88, respectively. Although characterized by fairly variable $(La/Yb)_N$ ratios, basalts from the North Apennine Internal Ligurides (Venturelli et al., 1981; Ottonello et al., 1984) and Corsica (Venturelli et al., 1981), display ratios that are generally lower than those observed in the Hellenic-Dinaric belt and South Apuseni Mts ophiolites.

One of the major point of difference between South Apuseni Mts and Sava-Vardar Zone ophiolites is the widespread occurrence of ultramafic bodies in the latter (Pamic et al., 2002 and references therein). Nonetheless, Bortolotti et al. (2002) suggested that the lack of ultramafics in the South Apuseni Mts ophiolites may result from significant post-obduction tectonic movements.

CONCLUSIONS

In summary, all the geological and geochemical data suggest a strict correlation of the South Apuseni Mts ophiolites with those of the Sava-Vardar Zone of the Hellenic-Dinaric belt.

Therefore, the South Apuseni Mts ophiolites can be regarded as a fragment of the Vardar oceanic basin emplaced onto the continental margin of the Adria plate during the Late Jurassic-Early Cretaceous time span. The continous convergence resulted in the Late Cretaceous – Early Tertiary in a continental collision, mainly driven by the relative northward motion of the Adria plate with respect to the stable European continental plate. In the Early Tertiary the deformation was probably intracontinental, although some oceanic domains could have been still opened during the Late Eocene time (Schmid et al., 1998, Linzer et al., 1998; Neugebauer et al., 2001). In the Late Paleogene – Early Neogene, the convergence between the Adria microplate and Eastern European plate, probably combined with the retreat of the subducting European margin, produced not only shortening and thickening in the Carpathian belt, but also transpressive tectonics connected with the eastward escape and rotation of the Alcapa and Tisza rigid blocks. In this framework (Fig.12), the Tisza and Alcapa blocks probably were originated as separate microplates, which subsequently rotated and translated independently from each other along the main transpressive lines identified in the Pannonian basin (see for instance the reconstructions of Csontos, 1995 and Neugebauer et al., 2001). The present-day location in the hinterland of the Carpathian area achieved in the the Late Paleogene – Early Neogene time span, when the escape tectonics produced a large-scale displacement of blocks originated from the northernmost edge of the Adria plate. Among them, the Tisza block is characterized by a stack of continental and oceanic tectonic units derived from the Adria continental margin and the neighbouring Vardar basin, with the latter represented by the South Apuseni Mts ophiolites which are displaced about 300 km eastward with respect to the northernmost Vardar ophiolites (Bortolotti et al., 2002).

On the whole, the South Apuseni Mts ophiolites can be regarded as originally located in the northern continuation

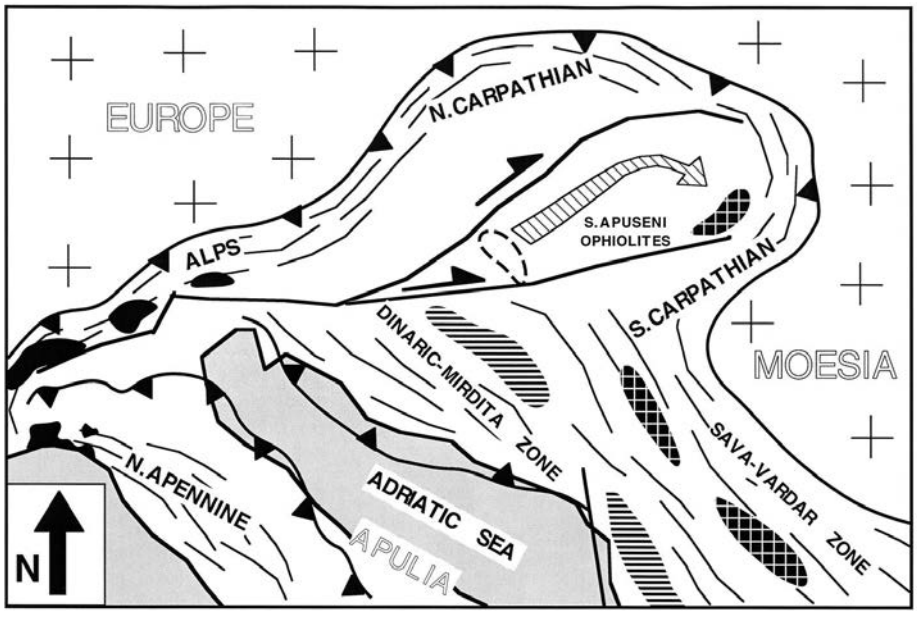

Fig. 12 - Sketch of the tectonic setting of the Alpine-Carpathian areas with theirs main ophiolitic zones. The probable trajectory of the South Apuseni Mts. during the Neogene is indicated. The strike-slip faults that bounded the Tisza block are also shown.

of the Vardar oceanic domain, as suggested by the geological and petrological data presented in this paper.

ACKNOWLEDGEMENTS

This research was supported by M.I.U.R. COFIN, Institutul de Geodinamica al Academiei Romane, and Istituto di Geoscienze e Georisorse, CNR, Italy. Many thanks go to V. Hoeck and V. Morra, whose reviews greatly improved the manuscript.

REFERENCES

Abbate E., Bortolotti V. and Principi G., 1980. Apennine ophiolites: a peculiar oceanic crust. In: G.Rocci Ed. Special Issue on Tethyan ophiolites, vol.I, western area, Ofioliti, 5: 59-96.

Bebien J., Baroz F., Capedri S. and Venturelli G. 1987. Magmatismes basiques associes à l'overture d'un bassin marginal dans les Hellenides internes au Jurassique. Ofioliti, 12: 53-70.

Beccaluva L., Macciotta G., Piccardo G.B. and Zeda O., 1989. Clinopyroxene compositions of ophiolite basalts as petrogenetic indicator. Chemical Geology, 77: 165-182.

Bleahu M., Lupu M., Patrulius D., Bordea L., Stefan A. and Panin S., 1981. Guide to the excursion, B3: the structures of the Apuseni Mts. Carpatho-Balcan Geological Association XII Congress, Bucharest, Romania: 80pp.

Bleahu M., Soroiu M. and Catilina R., 1984. On the Cretaceous tectono-magmatic evolution of the Apuseni Mountains as revealed by K-Ar dating. Rev. Roum. Phys., 29: 123-130.

Bortolotti V., Marroni M., Nicolae I., Pandolfi L., Principi G. and Saccani E., 2002. Geodynamic implications of Jurassic ophiolites associated with island-arc volcanics, South apuseni Mountains, Western Romania. Int. Geol. Rev., 44: 938-955.

Burchfiel B.C., 1980. Eastern european alpine system and the Carpathian orocline as an example of collision tectonics. Tectonophysics 63: 31-61.

Cioflica G., Lupu M., Nicolae I., and Vlad S., 1980. Alpine ophiolites of Roumania: tectonic setting, magmatism and metallogenesis. An. Ist. Géol. Géophys., 56: 79-95.

Cioflica G., Lupu M., Nicolae I., Lupu M., Vlad S., 1981. Guide to excursion A3: Alpine ophiolitic complexes in south Carpatian and south Apuseni Mountains. Carpatho-Balcan Geological Association XII Congress, Bucharest, Romania: 80pp.

Cioflica G. and Nicolae I., 1981. The origin, evolution and tectonic setting of the Alpine ophiolites from the South Apuseni Mountains. Rev. Roum. Géol. Géophys. Géogr., 25: 19-29.

Csontos L., 1995. Tertiary tectonic evolution of the intra-carpathian area: a review. Acta Vulcanologica, 7(2): 1-13.

Dallmeyer R.D., Pana D.I., Neibauer F. and Erdmer P., 1999. Tectonothermal evolution of the Apuseni Mountains, Romania: resolution of Variscan versus Alpine events with 40AR/39Ar ages. Journal of Geology, 107: 329-352.

Dal Piaz G.V., Martin S., Villa I.M. and Gosso G., 1995. Late Jurassic blueschist facies pebbles from the Western carpathians orogenic wedge and paleostructural implications for Western Tethys evolution. Tectonics, 14(4): 874-885.

Danelian T., Robertson A.H.F. and Dimitriadis S., 1996. Age and significance of radiolarian sediments within basic extrusive of the marginal basin Guevgueli Ophiolite (northern Greece). Geol. Magaz., 133: 127-136.

De Paolo D.J., 1981. Trace element and isotopic effects of combined wallrock assimilation and fractional crystallization. Earth Planet. Sci. Letters, 53: 189-202.

Dercourt J., Ricou L.E., Adamia S., Csazsar G., Funk H., Lefeld J., Rakus M., Sandulescu M., Tollman A. and Tchoumachenko P., 1990. Anisian to Oligocene paleogeography of the European margin of Tethys (Geneva to Baku). Mém. Soc. Géol. Fr., 154(3): 159-190.

Ellero A., Leoni L., Marroni M., Pandolfi L. & Sartori F., 2002. Deformation and metamorphism in the Fenes Nappe (Southern Apuseni Mountains, northern Romania). Compte Rendu Geoscience, 334(5): 347-354

Ivanov T., Misar Z., Bowes D.R., Dudek A., Dumurdzanov N., Jaros J.J., Elinek E. and Pacesova M., 1987. The Demir Kapija-Gevgelija ophiolite massif, Macedonia, Yugoslavia. Ofioliti, 12(3): 457-478.

Hildreth W. and Moorbath S., 1988. Crustal contribution to arc magmatism in the Andes of Central Chile. Contrib. Minaralogy and Petrology, 98: 455-489.

Horvath F. and Royden L., 1981. Mechanism for the formation of the intra-Carpathian basins: a review. Earth Evol. Sci., 3: 307-316.

Kovacs S., 1982. Problems of the "Pannonian Median Massif" and the plate tectonic concept. Contribution based on the distribution of Late Paleozoic – Early Mesozoic isopic zones. Geol. Rund., 71: 617-640.

Leterrier J., Maury R.C., Thonon P., Girard D. and Marchal, M., 1982. Clinopyroxene composition as a method of identification of the magmatic affinities of paleo-volcanic series. Earth Planet. Sci. Letters, 59: 139-154.

Linzer H.G., 1996. Kinematics of retreating subduction along the Carpathian area. Geology, 24: 167-170.

Linzer H.G., Frisch W., Zweigel P., Girbacea R., Hann H.P. and Moser F., 1998. Kinematic evolution of the Romanian Carpathians. Tectonophysics, 297: 133-156.

Lugovic B., Altherr R., Raczek I., Hofmann A.W. and Majer V., 1991. Geochemistry of peridotites and mafic igneous rocks from the Central Dinaric Ophiolite Belt, Yugoslavia. Contrib. Mineral. Petrol., 106: 201-216.

Lupu M., 1976. The main tectonic features of the Southern Apuseni Mts. Rev. Roum. Géol. Géophys. Géogr., 20: 21-25.

Lupu M., 1983. The Mesozoic history of the South Apuseni Mountains. An. Ist. Geol. Geophys., 60: 115-124.

Lupu M., Antonescu E., Avram E., Dumitrica P. and Nicolae I., 1995. Comments on the age of some ophiolites from the north Drocea Mts. Rom. J. Tect. & Reg. Geol., 76: 21-25.

Marton E., Pagac P. and Tunyi I., 1992. Paloemagnetic investigations on late Cretaceous-cenozoic sediments from the NW part of the Pannonian basin. Geol. Carphatica, 43: 363-369.

Miyashiro A., 1974. Volcanic rock series in island arcs and active continental margins. Am. J. Science, 274: 321-355.

Neugebauer J., Greiner B. and Appel E., 2001. Kinematics of the Alpine-West Carpathian orogen and paleogeographic implications. Journ. Geol. Soc. London, 158: 97-110.

Nicolae I., 1995. Tectonic setting of the ophiolites from the South Apuseni Mountains: magmatic arc and marginal basin. J. Tect. & Reg. Geol., 76: 27-38.

Nicolae I., Cuna S. and Soroiu M., 1987. Preliminary K-Ar investigations of ophiolites from the South Apuseni Mountains (Romania). Stud. cerc. Geol. Geofiz. Geogr. Geofizica, 25: 43-49.

Nicolae I., Soroiu M. and Bonhomme G.M., 1992. Ages K-Ar de quelques ophiolites des Monts Apuseni du sud (Roumanie) et leur signification géologique. Géologie Alpine, 68: 77-83.

Nicolae I. and Saccani E., 2003. Petrology and geochemistry of the Late Jurassic calc-alkaline series associated to Middle Jurassic ophiolites in the South Apuseni mountains (Romania). Swiss Bull. Mineral. Petrol., 83: 81-96.

Ottonello G., Joron J.L. and Piccardo G.B., 1984. Rare Earth and 3d transition element geochemistry of peridotitic rocks: II. Ligurian peridotites and associated basalts. Jour. Petrol., 25: 373-393.

Pearce J.A., 1983. Role of the Sub-continenetal Lithosphere in Magma Genesis at Active Continental Margin. In: C.J. Hawkesworth and M.J. Norry (Editors), Continental basalts and mantle xenoliths. Shiva, Nantwich: 230-249.

Pamic J., Tomljenovic B. and Balen D., 2002. Geodynamic and petrographic evolution of Alpine ophiolites from the central and NW Dinarides: an overview. Lithos, 65: 113-142.

Pana D.I., 1998. Petrogenesis and tectonic of the basement rocks of the Apuseni Mountains: significance for the alpine tectonic of the Carpathian-Pannonian region. PHD thesis, Univ. of Alberta (Canada), Dept. of earth and atmospheric Science, Edmonton, 356pp.

Ratschbacher L., Linzer H.G. and Moser F., 1993. Cretaceous to Miocene thrusting and wrenching along the Central South Carpathians due to a corner effect during collision and orocline formation. Tectonics, 12: 855-873.

Robertson A.H.F., 1994. Role of the tectonic facies concept in orogenic analysis and its application to Tethys in the Eastern Mediterranean region. Earth Sci. Rev., 37: 139-213.

Royden L., 1993. Evolution of retreating subduction boundaries formed during continental collision. Tectonics, 12: 629-638.

Saccani E., Nicolae I. and Tassinari R., 2001. Tectono-magmatic setting of the Jurassic ophiolites from the South Apuseni mountains (Romania): Petrological and geochemical evidence. Ofioliti, 26: 9-22.

Sandulescu M., 1984. Geotectonica Romaniei. Edit. Tehn. Bucuresti, 336pp.

Sandulescu M., 1994. Overview on the Romanian geology. Rom. Jour. of Tectonics and Regional Geology, 75: 3-15.

Savu H., Udrescu C. and Neacsu V., 1981. Geochemistry and geotectonic setting of ophiolites and island arc volcanics of the Mures zone (Romania). Ofioliti, 6: 269-286.

Savu H. Udrescu C., Neacsu V. and Ichim M., 1994. Petrology and geochemistry of the Effusive rocks from the ocean floor basalt complex in the Mures Zone. Rom. J. Petrology, 76: 67-76.

Savu H., Grabari G. and Stoian M., 1996. New data concerning the structure, petrology and geochemistry of the Late Kimmerian granitoid massif of Savarsin (Mures Zone). Rom. Jour. Petrol., 77: 71-82.

Schmid S.M., Berza T. Vlad D., Froitzheim N. and Fugenschuh B., 1998. Orogen-parallel extension in the Southern Carpathians. Tectonophysics, 297: 209-228.

Serri G., 1981. The petrochemistry of ophiolite gabbroic complexes: a key for the classification of ophiolites into low-Ti and high-Ti types. Earth Planet. Sci. Letters, 52: 203-212.

Shervais J.W., 1982. Ti-V plots and the petrogenesis of modern ophiolitic lavas. Earth Planet. Sci. Letters, 59: 101-118.

Sun S.S. and McDonough W.F., 1989. Chemical and isotopic systematics of ocean basalts: Implications for mantle composition and processes. In: Magmatism in the Ocean Basins (A.D. Saunders and M.J. Norry, eds.), Geol. Soc. Spec. Publ., 42: 313-346.

Trubelja F., Marchig V., Burgath K.P., Vujovic Z., 1995. Origin of the Jurassic Tethyan Ophiolites in Bosnia: A Geochemical approach to tectonic setting. Geologica Croatica, 48: 49-66.

Venturelli G., Thorpe R.S. and Potts P.J., 1981. Rare earth and trace element characteristics of ophiolitic metabasalts from the Alpine-Apennine belt. Earth Planet. Sci. Letters, 53: 109-123.

Zacher W. and Lupu M., 1998. The ocean floor puzzle of the Alpine: Carpathian orogenic belt. Jahrb. Geol., 141: 97-106.

Received, March 15, 2004
Accepted, May 21, 2004